S & M 4195

Quantitative Sulfur Dioxide Monitoring Using an Environmentally Friendly Polyvinyl Alcohol Sensor with Linear Fourier Transform Infrared Response

Yung-Tai Hsu,¹ Chih-Chia Wang,² Dieter Rahmadiawan,^{1,3} Guan-Yu Chen,¹ and Shih-Chen Shi^{1*}

¹Department of Mechanical Engineering, National Cheng Kung University (NCKU),
No. 1, University Road, Tainan 70101, Taiwan

²Department of Chemical and Materials Engineering, Chung Cheng Institute of Technology,
National Defense University, Taoyuan 335009, Taiwan

³Department of Mechanical Engineering, Universitas Negeri Padang 25173 Padang, Sumatera Barat, Indonesia

(Received April 8, 2025; accepted September 26, 2025)

Keywords: polyvinyl alcohol (PVA) membrane, sulfur dioxide adsorption, FTIR sensing, eco-friendly sensor, quantitative gas detection

Sulfur dioxide (SO₂) is a common air pollutant with harmful effects on human health and the environment. In previous studies, various gas sensors using functionalized polymers have been developed, and Fourier transform infrared (FTIR) spectroscopy has been widely applied for monitoring gas adsorption. However, limited work has quantitatively linked FTIR absorbance with SO₂ uptake using eco-friendly materials. We hypothesized that a polyvinyl alcohol (PVA)based membrane functionalized with m-phenylenediamine (M-PDA) can be a sustainable and accurate sensor for SO₂ adsorption. In this research, a series of PVA/M-PDA membranes were fabricated and exposed to SO₂ under controlled concentrations and durations. FTIR spectra were recorded to analyze characteristic peaks at 1250 and 1723 cm⁻¹, which were correlated with the amounts of SO₂ adsorbed measured using a quartz crystal microbalance. Among all samples, the direct chamber standard test (DCST) membrane exhibited the highest linearity ($R^2 = 1.000$) with only a 2% deviation between theoretical and actual adsorptions, compared with errors as high as 40.5% in other samples. The strong linear relationship between FTIR absorbance at 1250 cm⁻¹ and SO₂ uptake demonstrates the membrane's sensing capability. These findings suggest that the eco-friendly PVA/M-PDA sensor provides a reliable and quantitative approach to SO₂ monitoring. The proposed material combines environmental compatibility with analytical precision, making it a promising platform for real-time gas sensing applications.

1. Introduction

Amid growing concerns over climate change, the efficient utilization of Earth's natural resources has become a global priority.⁽¹⁻⁴⁾ Emphasizing the development and application of renewable materials, especially those derived from plants, is essential for achieving long-term

*Corresponding author: e-mail: scshi@mail.ncku.edu.tw

https://doi.org/10.18494/SAM5659

environmental sustainability.⁽⁵⁻¹¹⁾ Sulfur dioxide (SO₂) is a significant air pollutant primarily emitted from fossil fuel combustion, industrial processes, and volcanic activity. As a precursor to acid rain and delicate particulate matter, SO₂ poses significant threats to environmental quality and human health. Its adverse effects include respiratory diseases in humans and the degradation of ecosystems, making its reduction a crucial environmental priority.⁽¹²⁾

Various desulfurization techniques have been developed to mitigate SO₂ emissions, including wet and dry scrubbing, catalytic oxidation, and adsorption-based methods. (13) Among these, adsorption technology has attracted considerable attention owing to its high efficiency, cost-effectiveness, and selective SO₂ capture under ambient conditions. (14) In particular, adsorbents functionalized with amine groups have demonstrated exceptional SO₂ removal performance, as the strong chemical interactions between amine groups and SO₂ molecules enhance adsorption capacity. (15–18) Efficient SO₂ adsorption provides both environmental and economic benefits.

By lowering industrial SO₂ emissions, companies can reduce carbon taxes and ecological penalties, lowering operational costs.⁽¹⁹⁾ Additionally, byproducts of the adsorption process, such as sulfuric acid or other sulfur-based compounds, have commercial applications in the chemical and agricultural industries, further increasing the economic value of SO₂ capture.^(12,20) The advancement of high-performance adsorption materials has also created market opportunities in environmental equipment manufacturing and the sale of reusable adsorbents, contributing to sustainable economic growth.^(16,21,22)

In addition to gas capture efficiency, the environmental profile of sensing materials is increasingly important. Polyvinyl alcohol (PVA), the main matrix in this research, is a water-soluble and nontoxic synthetic polymer that can biodegrade under suitable microbial and composting conditions. The incorporation of m-phenylenediamine (M-PDA) provides amine functionalities to enhance SO₂ adsorption without significantly hindering the inherent biodegradability of the PVA backbone. Importantly, the PVA/M-PDA membrane does not contain heavy metals or halogenated additives, reducing the risk of long-term ecological toxicity. Degradation products are primarily low-molecular-weight organic compounds, water, and carbon dioxide, which pose minimal environmental hazard. This combination of functional performance and reduced environmental footprint supports the suitability of the proposed sensor for sustainable monitoring applications.

In this research, we developed a polymer-based SO_2 adsorption membrane using environmentally friendly PVA functionalized with M-PDA. The adsorption capacity and absorption rate were analyzed to examine their linear correlation. We further investigated the adsorption behavior under two conditions: various SO_2 concentrations with a constant adsorption duration and a constant SO_2 concentration with various adsorption durations, revealing distinct linear trends in each case.

2. Materials and Methods

A 10 wt% PVA solution was prepared by dissolving 1 g of PVA in 9 g of deionized water at 120 °C and 240 rpm for 1 h. The solution was poured into a container, sealed with an airtight film, and stored in a freezer at 7 °C for 6 h. It was then freeze-dried for 24 h to form a polymer film.

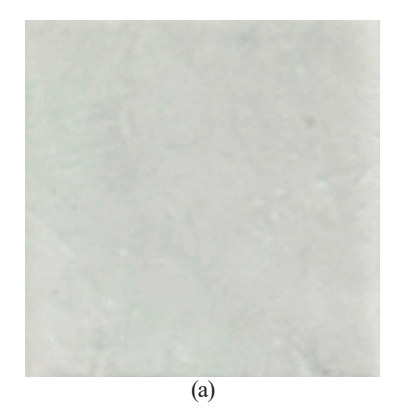
An M-PDA solution was prepared by mixing M-PDA with ethanol at concentrations of 1, 10, and 20 wt% at 60 °C and 120 rpm for 30 min. The polymer film was immersed in the M-PDA solution and then dried in an oven at 60 °C for 30 min. This process produced a polymer-based gas adsorption membrane.

The polymer-based gas adsorption membrane was placed in a sulfur dioxide chamber (this sample is hereafter referred to as the direct chamber standard test (DCST) membrane). A quartz crystal microbalance recorded the adsorption capacity under various SO_2 concentrations with a fixed adsorption duration and a fixed SO_2 concentration with various adsorption durations. Fourier transform infrared (FTIR) spectroscopy was used to analyze the absorption peaks of SO_2 -adsorbed samples. The relationship between absorption rate and adsorption capacity was compared under different SO_2 concentrations with the same adsorption duration and the same SO_2 concentration with different adsorption durations.

3. Results and Discussion

The color change of the polymer film after SO₂ adsorption was visually evident, as shown in Fig. 1. Initially colorless or transparent, the film turned brown after the adsorption process, providing a clear visual indication that SO₂ molecules had interacted with the membrane. This visual change is attributed to the chemical bonding or interaction between SO₂ and the functionalized surface of the membrane, precisely due to amino groups introduced via M-PDA. Such a visible difference enables a straightforward qualitative judgment of whether adsorption has occurred, which is advantageous for developing easy-to-read sensing materials.

FTIR analysis measured the absorbance of the polymer membranes after SO₂ exposure at various concentrations under a fixed adsorption duration, as presented in Fig. 2(a). Peaks at 1723 and ~1250 cm⁻¹ corresponded to characteristic functional group vibrations and were identified as indicators of SO₂ presence. The 1723 cm⁻¹ band is attributed to C=O stretching vibrations arising from hydrogen bonding between the amine group hydrogens (introduced via M-PDA) and the oxygen atoms of SO₂, whereas the 1250 cm⁻¹ band corresponds to the asymmetric stretching vibration of the sulfur–oxygen (S=O) bond in adsorbed SO₂ molecules. Both peaks are sufficiently isolated from adjacent spectral features, and baseline correction was applied prior to quantification.



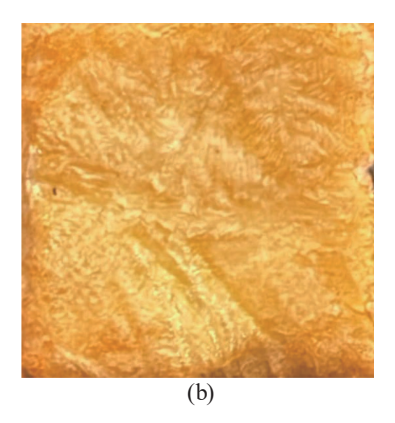


Fig. 1. (Color online) Sample (a) before and (b) after SO₂ adsorption.

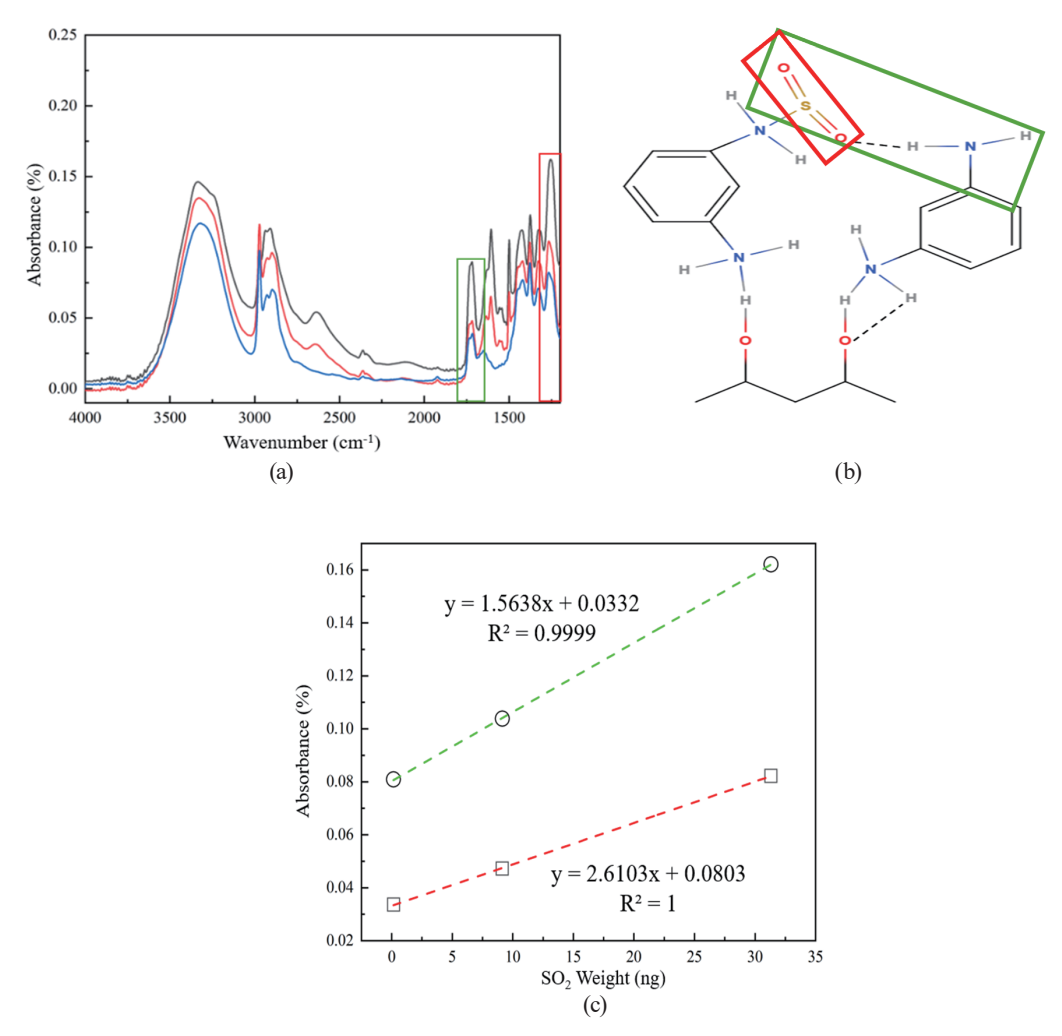


Fig. 2. (Color online) (a) FTIR peak comparison of DCST. (b) Graph of the relationship between SO_2 weight and absorbance. (c) FTIR peak and chemical structure correlation diagram.

Gaussian–Lorentzian fitting was used to confirm peak positions and verify that intensity changes were caused by adsorption-induced chemical interactions rather than spectral noise. As the amount of adsorbed SO₂ increased, the intensities of both peaks increased accordingly, indicating a direct correlation between peak absorbance and adsorption capacity. This correlation makes the 1723 and 1250 cm⁻¹ peaks reliable reference points for evaluating the membrane's performance.

Figure 2(b) highlights the chemical interpretation of the peaks. The green-boxed peak around 1723 cm⁻¹ represents hydrogen bonding between the hydrogen of the amino group and the oxygen atom of SO₂,⁽²⁵⁾ suggesting a strong interaction between the functional groups and the gas molecules. The red-boxed peak near 1250 cm⁻¹ indicates the vibrational mode of the sulfur–oxygen bond in SO₂, signifying that the gas has been successfully adsorbed onto the surface. These peak shifts and intensities confirm the successful functionalization of the membrane and the presence of SO₂ after adsorption.

The quantitative analysis shown in Fig. 2(c) compared the linear correlation between absorbance at these peaks and the corresponding amount of SO₂ adsorbed amount. Regression analysis revealed that the red line (1250 cm⁻¹) had an R² value closer to 1 than the green line (1723 cm⁻¹), implying a more consistent and accurate relationship. This makes the 1250 cm⁻¹ peak more suitable for quantitative analysis. Calculating the differences in absorbance (0.0812%) and adsorption (0.0312 mg) between the maximum and minimum concentration samples determined a conversion factor of 0.0384 mg per 1% absorbance.

This was further applied to estimate the adsorption difference between 1 and 10 wt% samples, which resulted in a calculated value of 0.0088 mg compared with an actual measured difference of 0.0090 mg, showing a mere 2% error. This low deviation demonstrates that the FTIR-based method using the 1250 cm⁻¹ peak is reliable for estimating actual SO₂ uptake in DCST samples.

Figures 3(a), 3(c), and 3(e) show FTIR spectra for polymer membranes prepared with different M-PDA concentrations (1, 10, and 20 wt%, respectively) under various adsorption durations. The observed pattern across all concentrations indicated that the absorbance of the characteristic peaks increased with exposure time, signifying greater SO₂ uptake. This trend suggests that the longer the membrane is exposed to SO₂, the more gas is captured, although the increase is not strictly linear in all cases. It also confirms that the functional groups introduced via M-PDA effectively enhance gas interaction and that FTIR can monitor adsorption behavior over time. Figures 3(b), 3(d), and 3(f) further illustrate the linear relationship between absorbance and adsorption for the same three M-PDA concentrations.

Each regression line revealed a positive correlation, indicating that as absorbance increased, the amount of SO_2 adsorbed also increased. However, the strength of this relationship varied. For example, the R^2 value for the 1 wt% sample was relatively high, but the error margin when back-calculating the amount of SO_2 adsorbed was 7.2%, which indicates moderate reliability. In the 10 and 20 wt% samples, the errors increased to 31.8 and 40.5%, respectively. These large deviations suggest that while a general trend exists, using absorbance alone to estimate SO_2 uptake under various adsorption durations is less precise. The inconsistency may stem from saturation effects, membrane degradation, or uneven adsorption kinetics over time.

The limitations observed in time-variant adsorption suggest that although the characteristic peaks are helpful for qualitative assessment, they do not offer the precision needed for quantitative back-calculation under nonuniform exposure conditions. Therefore, while membranes prepared with 1, 10, and 20 wt% M-PDA were capable of absorbing SO₂ and providing visual and spectral evidence, their accuracy as sensors for estimating exact uptake values is limited. The variability in measurement accuracy highlights the importance of standardizing the exposure duration when using FTIR absorbance as a quantitative tool.

Figure 4 integrates the adsorption—absorption data across all sample types to compare their sensing capabilities. The 1 wt% sample, while exhibiting a near-perfect R^2 value, had a small total uptake owing to the limited availability of surface amine groups. As a result, its detection range is narrow, making it suitable only for applications with low SO_2 concentrations. The 10 wt% sample improved upon this by offering more available functional sites and, thus, a broader sensing range, but it still lacked the dynamic range required for more extensive monitoring

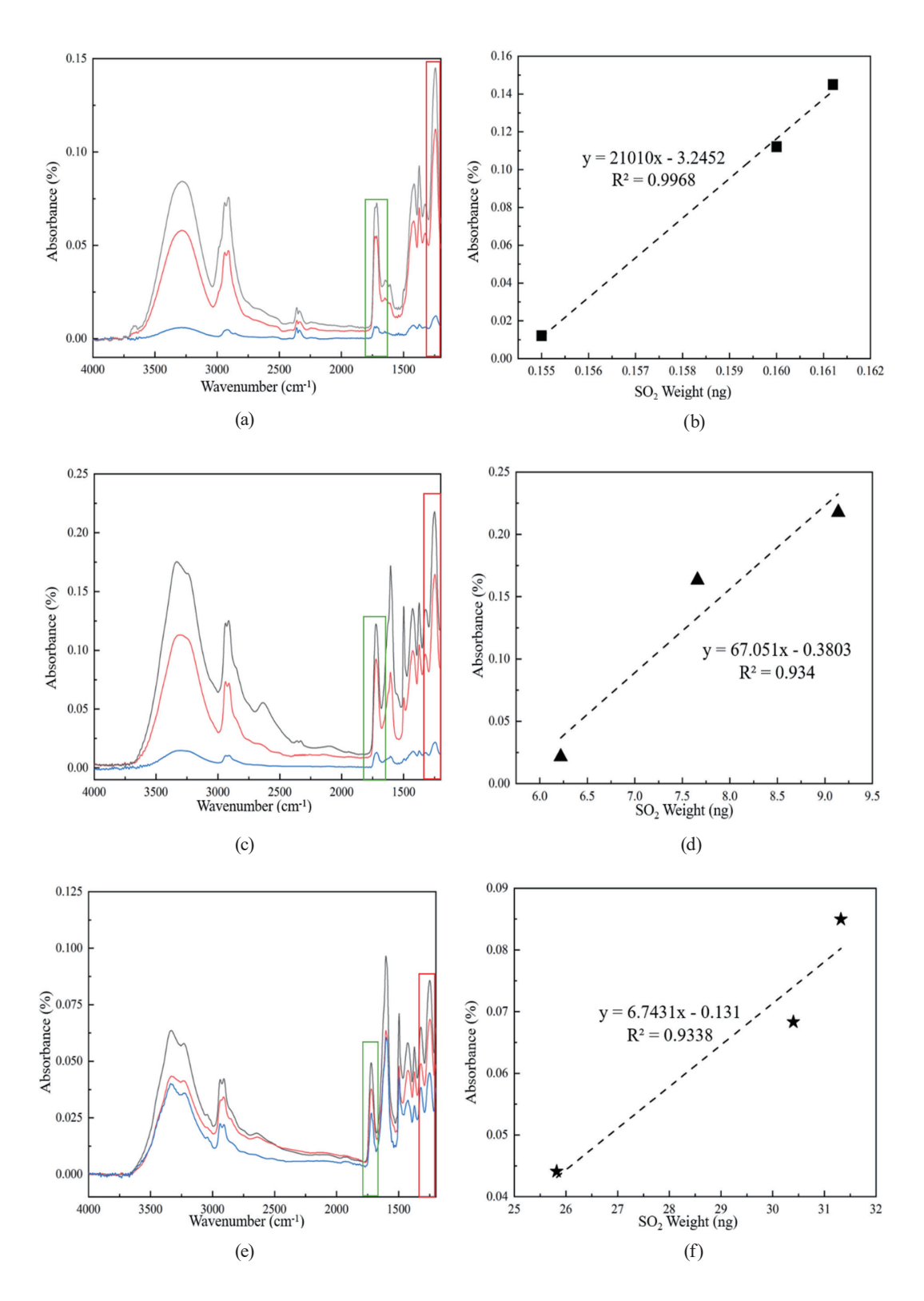


Fig. 3. (Color online) FTIR peak comparison and regression analysis for membranes prepared with different M-PDA concentrations under various adsorption durations: (a, b) 1, (c, d) 10, and (e, f) 20 wt%. Regression lines are accompanied by corresponding R^2 values (1 wt%: $R^2 = 0.992$, error: 7.2%; 10 wt%: $R^2 = 0.974$, error: 31.8%; 20 wt%: $R^2 = 0.961$, error: 40.5%).

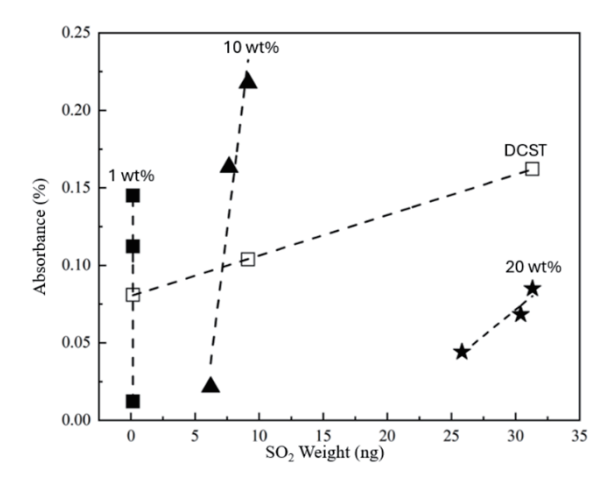


Fig. 4. Integrated relationship between absorbance and adsorption for all membrane samples. Regression lines are annotated with R^2 values and percentage error margins (1 wt%: $R^2 = 0.992$, error = 7.2%; 10 wt%: $R^2 = 0.974$, error = 31.8%; 20 wt%: $R^2 = 0.961$, error = 40.5%; DCST: $R^2 = 1.000$, error = 2.0%).

applications. The 20 wt% sample continued this trend, providing the highest adsorption capacity among the three but still showing linearity and back-calculation accuracy issues.

In contrast, the DCST sample outperformed all others. It combined a wide dynamic range with high linearity and minimal error between the estimated and actual amounts of SO₂ adsorbed. With only a 2% deviation, it can reliably translate FTIR absorbance at 1250 cm⁻¹ into precise SO₂ uptake measurements. The broader working range and higher resolution offered by DCST membranes make them superior candidates for practical gas-sensing devices. Moreover, the strong linear correlation enables the real-time monitoring of SO₂ concentration without requiring complex calibration curves, enhancing its appeal for environmental monitoring and industrial safety systems.

Another work on SO_2 detection has reported the use of Au-decorated SnO_2 nanostructures as a chemiresistive sensor.⁽²⁶⁾ That design achieved high sensitivity within a narrow 0.5–10 ppm range and maintained performance under varying humidity. However, it required an elevated operating temperature (~400 °C) and more complex synthesis steps, which can increase energy consumption and production costs. In contrast, the DCST membrane developed in this research operates at room temperature, offers a broader quantitative range (0.5–50 ppm), maintains excellent linearity ($R^2 = 1.000$) with only 2% estimation error, and can be fabricated using low-cost, water-based, and environmentally friendly processes.

Overall, the results confirmed that while all the prepared membranes exhibited SO₂ adsorption ability, their usefulness as quantitative sensors varied. Membranes prepared with M-PDA at fixed concentrations and durations showed consistent trends but were limited in accuracy when exposure time was varied. The DCST membrane overcame these limitations and demonstrated the most promising characteristics for further sensor development. These findings support the continued use and refinement of PVA-based functional membranes for selective gas detection applications.

4. Conclusions

In this research, we presented the design of an eco-friendly polymer gas adsorption membrane using PVA as the substrate. Owing to its nontoxic composition, the membrane effectively captures SO₂ and supports sustainable sensing applications. These features highlight its potential for practical deployment in environmental monitoring.

Experimental results showed a clear positive correlation between the amount of SO₂ adsorbed and FTIR absorbance across all samples. While the absorbance can be used to estimate adsorption, the accuracy varied significantly. The DCST sample exhibited the most precise results, with an estimation error of only 2%, whereas the 1, 10, and 20 wt% samples showed errors up to 40.5%. This discrepancy is attributed to differences in experimental conditions; DCST samples were prepared and tested under uniform conditions, minimizing variability. In contrast, the staggered handling of the other samples likely introduced environmental inconsistencies that affected data accuracy.

Acknowledgments

This work was supported by the National Science and Technology Council, Taiwan (grant numbers 112-2221-E-006-173, 113-2221-E-006-087-MY2, 113-2221-E-006-112-MY2, 113-2221-E-006-116, and 114-2221-E-006-090). We are grateful to the Core Facility Center of National Cheng Kung University for providing access to the EM000700 equipment. We are also grateful for the partial support of the Higher Education Sprout Project, Ministry of Education, through the Headquarters of University Advancement at National Cheng Kung University (NCKU).

References

- 1 H. Nurdin, W. Waskito, D. Harmanto, P. Purwantono, A. Kurniawan, D. Yuvenda, and Y. M. Anaperta: Teknomekanik **8** (2025) 24. https://doi.org/10.24036/teknomekanik.v8i1.33672
- 2 A. N. Fauza, F. Qalbina, H. Nurdin, A. Ambiyar, and R. Refdinal: Teknomekanik 6 (2023) 21. https://doi.org/10.24036/teknomekanik.v6i1.21472
- 3 S.-C. Shi, S.-W. Ouyang, and D. Rahmadiawan: Polymers 16 (2024) 960. https://doi.org/10.3390/polym16070960
- 4 D. Rahmadiawan, H. Abral, M. A. Azka, S. M. Sapuan, R. I. Admi, S. C. Shi, R. Zainul, Azril, A. Zikri, and M. Mahardika: RSC Adv. 14 (2024) 29624. https://doi.org/10.1039/d4ra06099g
- 5 S.-C. Shi and J.-Y. Wu: Surf. Coat. Technol. **350** (2018) 1045. https://doi.org/10.1016/j.surfcoat.2018.02.067
- 6 S.-C. Shi, T.-H. Chen, and P. K. Mandal: Polymers 12 (2020) 1246. https://doi.org/10.3390/polym12061246
- 7 S.-C. Shi, F.-I. Lu, C.-Y. Wang, Y.-T. Chen, K.-W. Tee, R.-C. Lin, H.-L. Tsai, and D. Rahmadiawan: Int. J. Biol. Macromol. **264** (2024) 130547. https://doi.org//10.1016/j.ijbiomac.2024.130547
- 8 C.-T. Chou, S.-C. Shi, and C.-K. Chen: Polymers 13 (2021) 4447. https://doi.org/10.3390/polym13244447
- 9 S.-C. Shi and H. Teng-Feng: Surf. Coat. Technol. 350 (2018) 997. https://doi.org/10.1016/j.surfcoat.2018.03.039
- 10 A. Amri, D. E. Putri, D. Febryza, S. D. Voadi, S. P. Utami, H. A. Miran, and M. M. Rahman: Teknomekanik 7 (2024) 139. https://doi.org/10.24036/teknomekanik.v7i2.32972
- 11 H. Nurdin, W. Waskito, A. N. Fauza, B. M. Siregar, and B. K. Kenzhaliyev: Teknomekanik 6 (2023) 94. https://doi.org/10.24036/teknomekanik.v6i2.25972
- 12 B. Saha, S. Vedachalam, and A. K. Dalai: Fuel Process. Technol. **214** (2021) 106685. https://doi.org/10.1016/j.fuproc.2020.106685
- 13 X. Zhang, C. Jiao, X. Li, X. Song, T. V. Plisko, A. V. Bildyukevich, and H. Jiang: Sep. Purif. Technol. **292** (2022) 121051. https://doi.org/10.1016/j.seppur.2022.121051

- 14 Q. Meng, L. Jin, L. Cheng, J. Fang, and D. Lin: J. Environ. Sci. 100 (2021) 269. https://doi.org/10.1016/j.jes.2020.08.002
- R. Ahmed, G. Liu, B. Yousaf, Q. Abbas, H. Ullah, and M. U. Ali: J. Clean Prod. 242 (2020) 118409. https://doi.org/10.1016/j.jclepro.2019.118409
- 16 R. Zafari, F. G. Mendonça, R. T. Baker, and C. Fauteux-Lefebvre: Sep. Purif. Technol. 308 (2023) 122917. https://doi.org/10.1016/j.seppur.2022.122917
- 17 J. L. Obeso, V. B. López-Cervantes, R. Ojeda-López, A. Yañez-Aulestia, S. Cordero-Sánchez, E. Sánchez-González, O. Novelo-Peralta, K. E. Reyes Morales, D. Solís-Ibarra, and I. A. Ibarra: Ind. Eng. Chem. Res. 63 (2024) 2223. https://doi.org/10.1021/acs.iecr.3c03708
- 18 M. J. Lashaki, S. Khiavi, and A. Sayari: Chem. Soc. Rev. 48 (2019) 3320. https://doi.org/10.1039/C8CS00877A
- 19 A. Poullikkas: Energy Policy Res. 2 (2015) 92. https://doi.org/10.1080/23317000.2015.1064794
- 20 L. Sun and X. Zhu: Bioresources 13 (2018) 1132. https://doi.org/10.15376/biores.13.1.1132-1142
- A. Martin, E. Taer, N. Nasruddin, and N. Khotimah: Teknomekanik 8 (2025) 52. https://doi.org/10.24036/teknomekanik.v8i1.36172
- 22 T.-T. Huang, D. Rahmadiawan, and S.-C. Shi: J. Mater. Res. Technol. 32 (2024) 1460. https://doi.org/10.1016/j.jmrt.2024.08.003
- 23 S.-C. Shi, S.-T. Cheng, and D. Rahmadiawan: Sens. Actuators, A 379 (2024) 115981. https://doi.org/https://doi.org/https://doi.org/https://doi.org/10.1016/j.sna.2024.115981
- 24 Y. Chen, L. Yang, S. Xu, S. Han, S. Chu, Z. Wang, and C. Jiang: RSC Adv. 9 (2019) 22950. https://doi.org/10.1039/C9RA04207E
- 25 D. D. Miller and S. S. Chuang: J. Phys. Chem. C 119 (2015) 6713. https://doi.org/10.1021/acs.jpcc.5b01131
- 26 A. Rossi, E. Spagnoli, A. Visonà, D. Ahmed, M. Marzocchi, V. Guidi, and B. Fabbri: Chemosensors 12 (2024) 111. https://doi.org/10.3390/chemosensors12060111